environmental microbiology

Environmental Microbiology (2020) **00**(00), 00–00 doi:10.1111/1462-2920.15180

Major changes in grapevine wood microbiota are associated with the onset of esca, a devastating trunk disease

Emilie Bruez,[1,2,3*] Jessica Vallance,[1,2] Angélique Gautier,[4] Valérie Laval,[4] Stéphane Compant,[5] Wolfgang Maurer,[5] Angela Sessitsch,[5] Marc-Henri Lebrun[4] and Patrice Rey[1,2]

[1]*INRAE, ISVV, UMR1065 Santé et Agroécologie du Vignoble (SAVE), Bordeaux Sciences Agro, Villenave d'Ornon, F-33140, France.*

[2]*Bordeaux Sciences Agro, INRAE, UMR1065 Santé et Agroécologie du Vignoble (SAVE), Gradignan, F-33130, France.*

[3]*Université de Bordeaux, Unité de recherche Œnologie, EA 4577, USC 1366 INRAE, Villenave d'Ornon, F-33882, France.*

[4]*INRAE, AgroParisTech, UMR 1290 Biologie et gestion des risques en agriculture (BIOGER), Thiverval-Grignon, F-78850, France.*

[5]*AIT Austrian Institute of Technology GmbH, Bioresources Unit, Center for Health & Bioresources, Tulln, 3430, Austria.*

Summary

Esca, a major grapevine trunk disease in old grapevines, is associated with the colonization of woody tissues by a broad range of plant pathogenic fungi. To identify which fungal and bacterial species are involved in the onset of this disease, we analysed the microbiota from woody tissues of young (10-year-old) grapevines at an early stage of esca. Using meta-barcoding, 515 fungal and 403 bacterial operational taxonomic units (OTUs) were identified in woody tissues. *In situ* hybridization showed that these fungi and bacteria co-inhabited in grapevine woody tissues. In non-necrotic woody tissues, fungal and bacterial microbiota varied according to organs and seasons but not diseased plant status. *Phaeomoniella chlamydospora*, involved in the Grapevine trunk disease, was the most abundant species in non-necrotic tissues from healthy plants, suggesting a possible non-pathogenic endophytic behaviour. Most diseased plants (70%) displayed cordons, with their central white-rot necrosis colonized essentially by two plant pathogenic fungi (*Fomitiporia mediterranea*: 60%–90% and *P. chlamydospora*: 5%–15%) and by a few bacterial taxa (*Sphingomonas* spp. and *Mycobacterium* spp.). The occurrence of a specific association of fungal and bacterial species in cordons from young grapevines expressing esca-foliar symptoms strongly suggests that that microbiota is involved in the onset of this complex disease.

Received 23 October, 2018; revised 22 July, 2020; accepted 31 July, 2020. *For correspondence. E-mail emilie.bruez@u-bordeaux.fr. Tel. +(33) 5 57 57 59 26; Fax: +(33) 5 57 57 58 13.

Introduction

Grapevine trunk diseases (GTDs) such as esca, *Eutypa* and *Botryosphaeria* diebacks have been a major concern in viticulture for the last two decades, resulting in huge economic losses (Calzarano *et al*., 2004; Mondello *et al*., 2018). Esca is associated with extensive necrosis of grapevine trunk and cordon woody tissues, as well as its typical foliar symptoms (reviews: Bertsch *et al*., 2013; Mondello *et al*., 2018). This slow evolving disease can lead to plant death (apoplexy) depending on plant physiology, climatic factors and cultural practices (Lecomte *et al*., 2012; Ouadi *et al*., 2019). This disease is associated with the colonization of wood tissues by unrelated plant pathogenic fungi such as *P. chlamydospora*, *P. minimum*, *N. parvum* and *D. seriata*, mainly isolated from black necrotic sectors or punctuations, whereas *F. mediterranea* is mostly isolated from white-rot necrotic tissues (Bertsch *et al*., 2013; Mondello *et al*., 2018). These GTD fungi are also found in woody tissues (necrotic and non-necrotic) of healthy grapevines. A statistical analysis of the occurrence of different types of necrosis in trunks from healthy and diseased grapevines (esca) highlighted a significant correlation between the amount of white-rot necrotic tissues and disease (Maher *et al*., 2012; Bruez *et al*., 2014). These observations suggested that fungi involved in the formation of white-rot

necrotic tissues could equally be involved in the development of this complex disease. Still, the inoculation of each GTD fungus to grapevine woody tissues, only induce local necrosis, in superficial and inner wood (Surico *et al*., 2006; Bertsch *et al*., 2013). When *D. seriata*, however, was inoculated to Tempranillo, a particularly susceptible cultivar, typical esca-foliar symptoms could be observed (Reis *et al*., 2016). These results suggest that several microorganisms are acting, either together or sequentially over several years, to cause this complex and slowly evolving disease.

Until now, only old grapevines (>15–25 years) expressing esca disease symptoms for many years have been monitored to identify which fungi colonized woody tissues. To study the wood microbiota associated with the onset of esca, we analysed young grapevines (10-year-old) that had been displaying esca symptoms for only a few years. Using classical microbiological isolation methods, bacterial and fungal species colonizing trunk and cordon woody tissues from these young grapevines were identified and their genetic diversity assessed using fingerprinting methods (Bruez *et al*., 2014; Bruez *et al*., 2015). GTD fungi were detected in necrotic and non-necrotic tissues from both healthy and diseased grapevines. As these microbiological isolation methods could display some technical bias, we decided to analyse the species composition of bacterial and fungal microbiota of these young grapevine woody tissues, using a culture-independent method such as meta-barcoding. This strategy allows an in-depth characterization of microbiota, including the detection of species difficult to cultivate, or only present at low abundance (Cuadros-Orellana *et al*., 2013). These techniques have been successfully applied to the analysis of fungal microbiota from grapevine woody tissues (Del Frari *et al*., 2019; Niem *et al*., 2020). In addition, we used *in situ* hybridization to localize fungi and bacteria in grapevine woody tissues. This strategy was efficient in determining the taxonomical composition of fungal and bacterial microbiota colonizing woody tissues (rootstock, trunk, and cordon) of either healthy or diseased grapevines. It also highlighted a specific microbial association colonizing white-rot necrotic tissues, specifically associated with esca disease.

Results

Experimental design and amplicon sequencing of fungal and bacterial microbiota from grapevine woody tissues

Our study was carried out on young (10-year-old) Cabernet Sauvignon grapevines (*Vitis vinifera* L.) from Luchey-Halde vineyard (Pessac Léognan, Bordeaux, France). This vineyard has been monitored for esca-foliar symptoms ever since its establishment in 2000. Plants were defined as diseased (symptomatic) if they had previously expressed esca-foliar symptoms at least twice over the last 4 years (2005–2009) before sampling (2010). Plants were defined as healthy (asymptomatic) if they had not displayed esca-foliar symptoms since 2000. The 28 samples corresponded to different woody tissues (non-necrotic or white-rot necrosis) from three different organs (rootstock, trunk, cordon) from either healthy or diseased grapevines sampled at different dates (April 2010, June 2010, September 2010, January 2011). Each sample corresponded to the pooling of woody tissues from four grapevines with similar characteristics (types of tissue, organ, date, healthy/diseased). Woody tissues from trunk and rootstock of diseased plants did not display any internal necrotic sectors. In 70% of diseased plants, a central white-rot necrosis, typical of esca, was observed only in the cordon. Such white-rot necrosis was never observed in trunks of diseased plants, or in the cordon and trunk of healthy plants (Bruez *et al*., 2014). Genomic DNAs were extracted from these woody tissues and analysed by amplicon-based meta-barcoding, using 454-pyrosequencing (fungi: ITS; bacteria: 16S). Overall, 226 432 fungal and 12 065 bacterial sequences were obtained from these 28 samples. After excluding singletons, 225 491 fungal sequences were clustered using QIIME (Caporaso *et al*., 2010), with a 97% similarity threshold, generating 515 fungal OTUs. These fungal OTUs corresponded mostly to *Ascomycota* (82%) and *Basidiomycota* (10.4%). After excluding singletons, 11 372 bacterial sequences were clustered using QIIME, generating 403 OTUs. These bacterial OTUs corresponded mostly to *Alphaproteobacteria* (33%), *Gammaproteobacteria* (25%) and *Actinobacteria* (17%). The order composition of these microbiota pooled for sampling dates are presented in Fig. 1A for fungi, and in Fig. 1B for bacteria. The main fungal microbiota orders were *Hypocreales* and *Pleosporales*, together representing 15% of all orders. For bacterial microbiota, *Rhizobiales*, *Actinomycetales* and *Xanthomonadales* were the most present in all samples.

Taxonomic diversity of fungal and bacterial microbiota of grapevine non-necrotic woody tissues

Alpha-biodiversity was calculated using all OTUs without singletons (Table 1). Values of Shannon indexes (Peet, 1974) ranged from 2.52 to 3.44 for fungal microbiota, while values of Simpson indexes (Peet, 1974) were lower than 0.93. These values showed that, although fungal communities were diversified, the number of abundant species was low: the 20 most abundant fungal OTUs (>0.8%), representing 20 different species, accounted for 83% of all fungal sequences. The values of Shannon indexes for bacterial communities ranged

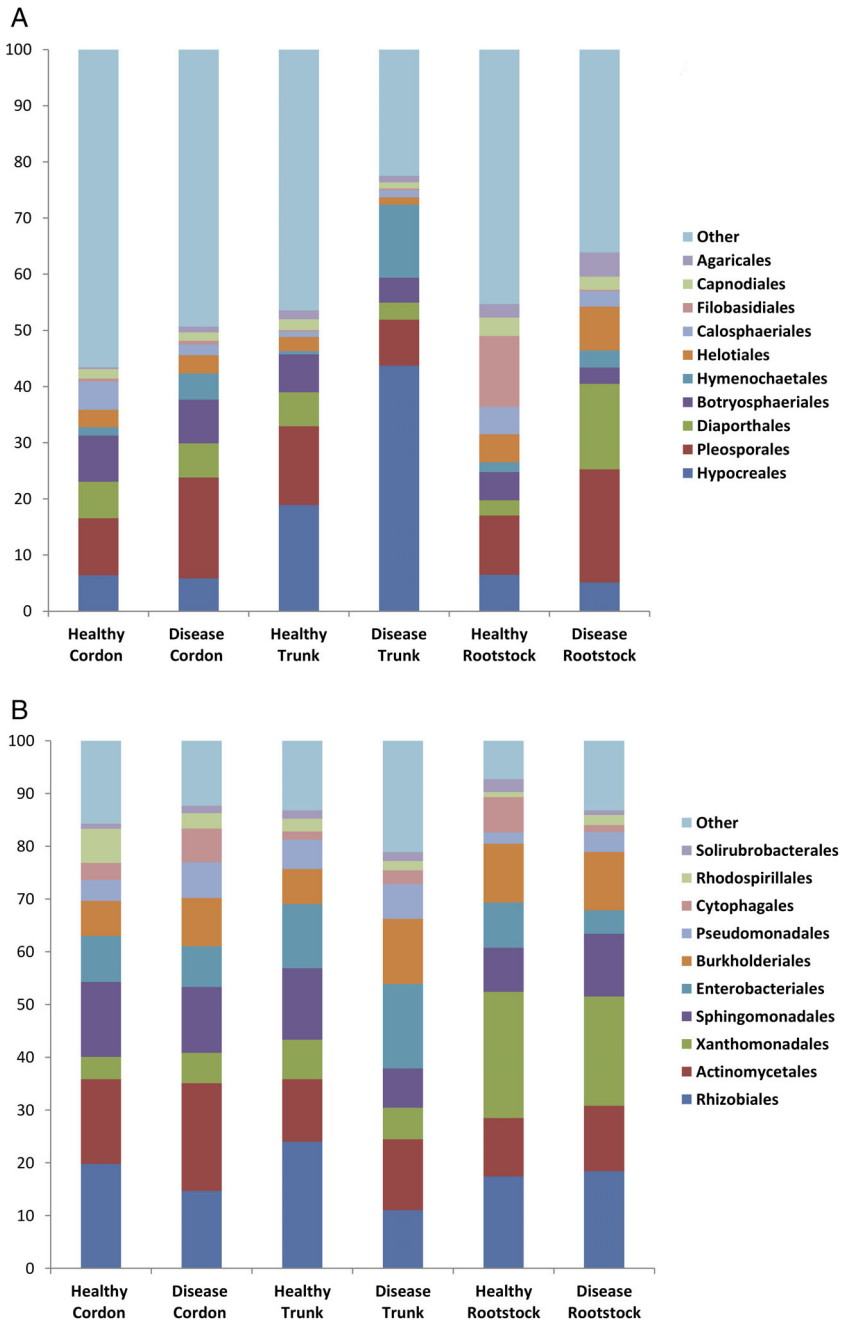

Fig 1. Meta-barcoding analysis of fungal (A) and bacterial (B) microbiota colonizing non-necrotic woody tissues from healthy and diseased young grapevines. DNAs were extracted from woody tissues of different organs (rootstock, trunk and cordon) from either healthy (asymptomatic) or diseased (symptomatic) young Cabernet-Sauvignon grapevines (10 -year-old) from a vineyard located at Pessac Léognan (Bordeaux, France). DNAs were used by amplicon-based meta-barcoding (fungi: ITS, bacteria: 16S). Only the 10 most abundant orders are displayed.

from 3.33 to 4.33, while values of Simpson indexes were lower than 0.98. Both values showed that bacterial communities were more diversified than fungal microbiota. This was reflected in the fact that the 20 most abundant bacterial OTUs (>1%), representing 20 different genera, only accounted for 60% of all bacterial reads, and 30 bacterial OTUs were needed to account for 83%. Rarefaction curves did not reach an asymptote suggesting that species either sampling was not sufficient or species saturation is difficult to reach in such a constrained environment (Supporting Information Fig. S1). Statistical analyses using values from different sampling dates as biological replicates, highlighted significant differences in Shannon and Simpson index values between fungal microbiota from necrotic (white-rot) and non-necrotic cordon tissues from diseased plants (Shannon index $P = 0.03$, Simpson index P value < 0.001; Table 1). As no significant differences were observed for other comparisons (Table 1), white-rot necrotic tissue of diseased plants displayed lower

Table 1. Diversity of esca-diseased and asymptomatic grapevine organs microbiota at, respectively, 3% and 1% genetic dissimilarity based on pyrosequencing of fungal (ITS) and bacterial (16 rRNA) communities.

		Non-necrotic rootstock	Non-necrotic trunk	Non-necrotic cordon	White-rot cordon
Shannon					
Healthy vines	Fungi	3.39 ± 0.25	3.44 ± 0.10	2.79 ± 0.54	
	Bacteria	3.33 ± 0.99	3.56 ± 0.32	4.08 ± 0.28	
Diseased vines	Fungi	3.29 ± 0.25	2.52 ± 0.47	2.77 ± 0.38	0.96 ± 0.37[a]
	Bacteria	4.00 ± 0.19	3.63 ± 0.38	4.33 ± 0.13	3.99 ± 0.29
Simpson					
Healthy vines	Fungi	0.92 ± 0.004	0.93 ± 0.01	0.81 ± 0.1	
	Bacteria	0.86 ± 0.01	0.95 ± 0.02	0.97 ± 0.01	
Diseased vines	Fungi	0.91 ± 0.04	0.80 ± 0.09	0.83 ± 0.06	0.41 ± 0.16[a]
	Bacteria	0.96 ± 0.01	0.94 ± 0.03	0.98 ± 0.004	0.96 ± 0.01

[a]Indicates significant differences, $\alpha < 5\%$, Chi square test, using sampling dates as biological replicates, $n = 4$.

fungal species diversity than in the case of neighbouring non-necrotic tissue.

Large-scale analysis of variations in the taxonomic composition of fungal and bacterial microbiota from different grapevine non-necrotic woody tissues

NMDS and ANOSIM analyses (Buttigieg and Ramette, 2014) were performed with all the OTUs identified in non-necrotic tissue without singletons, using a Bray–Curtis dissimilarity index as a distance (Fig. 2). The taxonomic compositions of fungal communities from non-necrotic tissues of healthy and diseased grapevines were similar (Fig. 2C; $P = 0.16$). Fungal species composition varied according to sampling dates (Fig. 2A; $P < 0.01$) and organs (Fig. 2B; $P < 0.01$). Comparison between pairs of organs, using an ANOVA with pooled data (sampling time, disease status), revealed that fungal microbiota of cordon significantly differed from those of trunk and rootstock (Table S1A; $P = 0.04$ and $P = 0.06$, respectively), while those of trunk and rootstock were similar (Table S1A; $P = 0.66$). The taxonomic compositions of bacterial communities from non-necrotic tissues of healthy and diseased grapevines were similar (Fig. 2F; $P = 0.22$). Bacterial taxonomical composition did not vary with sampling dates (Fig. 2D; $P = 0.243$). However, comparison between pairs of sampling dates using an ANOVA with pooled data (organs, disease status) revealed that bacterial microbiota sampled in January differed significantly from those of June (Table S1B; $P < 0.05$). Bacterial taxa composition also varied according to organ (Fig. 2E; $P = 0.006$). Comparison between pairs of organs, using an ANOVA with pooled data (sampling time, disease status), revealed that the bacterial microbiota of rootstock significantly differed from those of trunk and cordon (Table S1C; $P < 0.001$ and $P = 0.02$, respectively). Those of trunk and cordon were also statistically different (Table S1C; $P = 0.05$).

Variations in the taxonomic composition of fungal and bacterial microbiota from non-necrotic woody tissues according to organs and disease status

The twenty most abundant fungal species (> 0.8%) detected in non-necrotic woody tissues are presented in Table 2A (cordons) and Supporting Information Table S3 (all organs). The GTD fungus *P. chlamydospora* was the most abundant fungal species in non-necrotic woody tissues (average 30%, range 11%–62%). Other GTD fungi, such as *D. seriata*, *N. parvum*, *P. minimum* and *F. mediterranea*, were also detected, but at lower abundances (3%–7.5%). Four fungal species not involved in GTDs (*Bionectria ochroleuca*, *Camarographim koreanum*, *Diaporthe eres*, *Microsphaeropsis arundinis*) were also detected in relatively high abundance (>5%). Among these four taxa, the two most abundant species were *M. arundinis* (10.8%) and *D. eres* (9.6%), described as common tree endophytes (Sieber, 2007; Sun *et al*., 2012; de Freitas Sia *et al*., 2013). Statistical analyses were performed for each fungal species using values from different sampling dates as biological replicates. In healthy plants, the relative abundances of three fungal species (*Aureobasidium pullulans*, *C. koreanum*, and *P. chlamydospora*) significantly differed between cordon and trunk (Supporting Information Table S2). *C. koreanum* and *P. chlamydospora* were more abundant in cordon (2.3- and 1.8-fold, respectively, Supporting Information Table S3), while *A. pullulans* was more abundant in trunk (2.6-fold, Supporting Information Table S3). In diseased plants, we did not detect significant differences in the relative abundance of fungal species between organs (Supporting Information Table S2). Comparisons of fungal microbiota between healthy and diseased plants were performed for each organ (Supporting Information Table S2), with an emphasis on cordon (Table 2A). We did not detect significant differences in the relative abundance of fungal species in rootstock and trunk between healthy and diseased plants. However, the

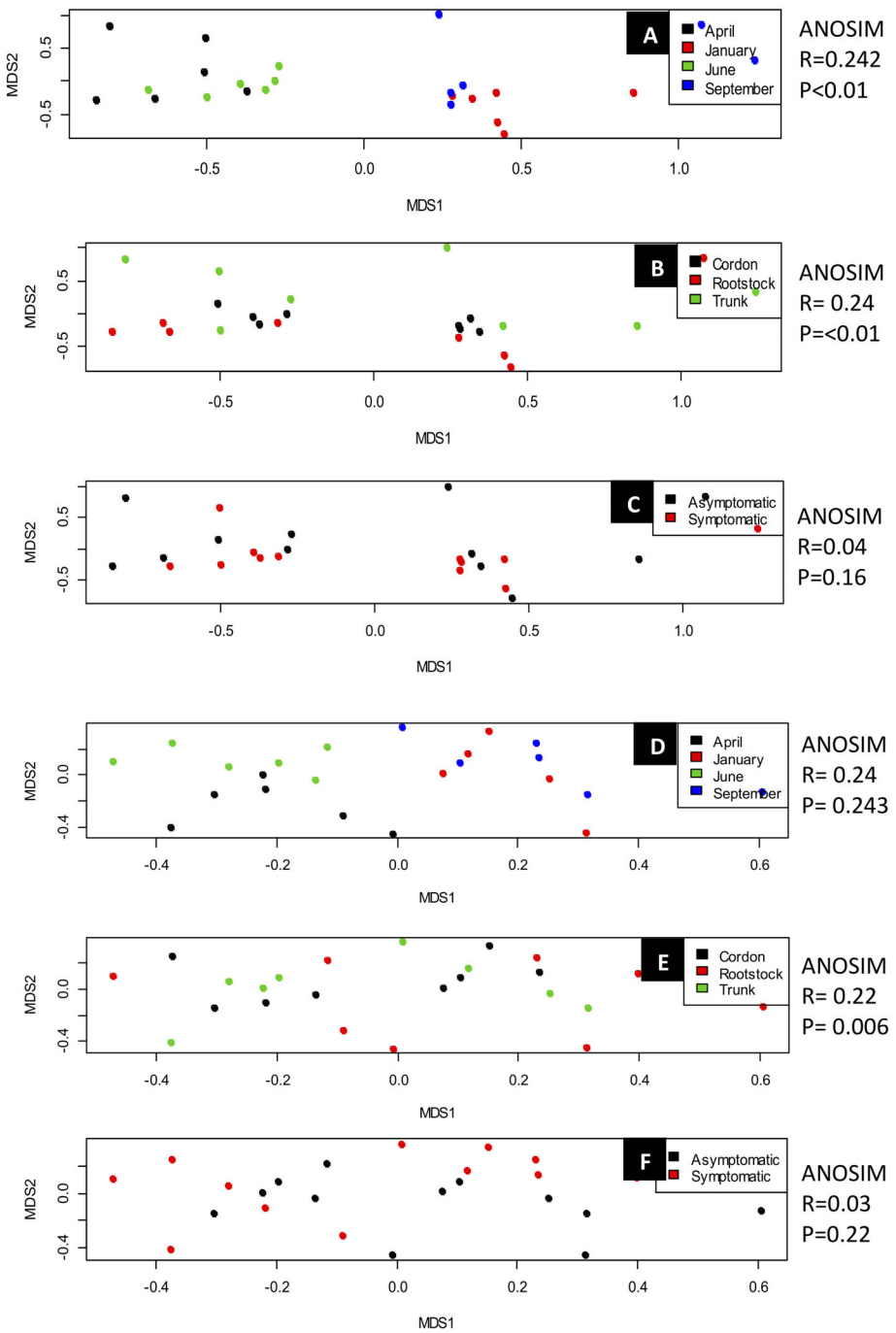

Fig 2. Comparison of the OTU composition of bacterial and fungal microbiota colonizing grapevine non-necrotic woody tissues using Non-metric multidimensional scaling (NMDS). NMDS analysis was based on Bray–Curtis dissimilarity indexes. Data used for this analysis contained all OTUs from meta-barcoding. ANOSIM test: Differences between parameters tested are significant if the *P*-value is <0.01.
A. Comparison of OTU compositions of grapevine non-necrotic woody tissues according to sampling dates (April, June, September, and January). Six replicates: three organs × two healthy/diseased status.
B. Comparison of fungal OTU compositions of grapevine non-necrotic woody tissues according to organs sampled (rootstock, trunk, and cordon). Seven replicates: four time points × two healthy/diseased status.
C. Comparison of fungal OTU compositions of grapevine non-necrotic woody tissues according to healthy (asymptomatic) and diseased (symptomatic) vines. Seven replicates: four time points × two healthy/diseased status.
D. Comparison of bacterial OTU compositions of grapevine non-necrotic woody tissues according to sampling dates (April, June, September, and January). Six replicates: three organs × two healthy/diseased status.
E. Comparison of bacterial OTU compositions of grapevine non-necrotic woody tissues according to organs sampled (rootstock, trunk, and cordon). Seven replicates: four time points × two healthy/diseased status.
F. Comparison of bacterial OTU compositions of grapevine non-necrotic woody tissues according to healthy (asymptomatic) and diseased (symptomatic) vines. Seven replicates: four time points × two healthy/diseased status.

relative abundances of two fungal species (*A. pullulans* and *P. chlamydospora*) differed in cordon between healthy and diseased plants (Supporting Information Table S2). *A. pullulans* and *P. chlamydospora* were more abundant in cordon from healthy than diseased plants (both onefold and fourfold, Table 2A). This observation suggested that these fungal species decreased in abundance in non-necrotic tissues from cordon during disease development.

The 20 most abundant bacterial genera (>1%) detected in non-necrotic woody tissues are presented in Table 2B (cordons) and Supporting Information Tables S4 (all samples). The most abundant bacterial families were the *Sphingomonadaceae* (15%–29%), *Enterobacteriaceae* (6%–22%) and *Rhizobiaceae* (6%–19%). Most bacterial families were composed of a few bacterial OTUs, with some assigned to a single genus or two genera (Supporting Information Table S4). For example,

Table 2. Proportions (%) of the 20 most abundant species of fungi (A) and bacteria (B) in the non-necrotic tissues of the cordon of healthy and diseased vines.

(A) Fungi	April		June		September		January		Mean	Mean	Statistics	Ratio
Specie	Healthy	Disease	Healthy	Disease	Healthy	Disease	Healthy	Disease	Healthy	Disease	*P*-value	WR/NN
Asterosporium betulinum	7.0	0.3	0.5	0.1	0.6	0.4	0.2	0.0	2.1	0.2	NS	0.11
Aureobasidium pullulans	1.8	1.1	2.4	0.9	3.7	3.4	1.8	1.2	2.4	1.7	0.001	0.69
Bionectria ochroleuca	0.1	10.2	6.2	0.5	0.9	0.4	0.2	0.0	1.9	2.8	NS	1.49
Camarographium koreanum	1.3	45.7	10.2	2.7	3.9	3.5	4.0	0.5	4.8	13.1	NS	2.71
Cladosporium cladosporioides	0.8	0.9	2.5	1.0	2.3	2.1	1.6	2.4	1.8	1.6	NS	0.89
Diaporthe eres	9.5	6.5	8.0	18.2	8.1	7.0	7.4	2.6	8.3	8.6	0.049	1.04
Diplodia seriata	1.5	2.4	1.7	1.5	2.4	2.6	2.1	19.8	1.9	6.6	NS	3.44
Epicoccum nigrum	1.0	0.3	1.1	0.7	0.0	0.2	0.1	0.0	0.5	0.3	NS	0.60
Fomitiporia mediterranea	2.8	5.3	0.1	13.1	6.6	4.3	0.0	3.3	2.4	6.5	NS	2.70
Lophiostoma cynaroidis	1.1	0.2	0.0	0.1	7.2	2.1	0.0	0.1	2.1	0.6	NS	0.30
Massarina rubi	0.4	0.3	0.6	0.4	1.1	0.8	3.1	0.1	1.3	0.4	NS	0.30
Microsphaeropsis arundinis	2.1	4.0	1.9	2.3	14.8	30.9	0.9	7.4	4.9	11.1	NS	2.27
Neofabraea malicorticis	1.2	0	1.5	2	0.5	0	2.7	6	1.5	2.2	NS	1.44
Neofusicoccum parvum	3.1	1.2	0.1	4.3	6.4	4.1	15.4	0.3	6.2	2.5	NS	0.40
Ochrocladosporium elatum	0.2	0.4	0.1	1.8	0.6	0.2	0.0	0.0	0.2	0.6	NS	2.86
Phaeoacremonium minimum	1.2	0.1	1.1	2.4	1.8	0.8	12.4	2.7	4.1	1.5	NS	0.37
Phaeomoniella chlamydospora	**62.1**	**15.3**	**56.6**	**39.4**	**32.9**	**29.6**	**41.2**	**50.9**	**48.2**	**33.8**	**0.021**	**0.70**
Phialophora sessilis	0.1	0.4	0.5	1.9	1.9	1.4	1.5	0.4	1.0	1.0	NS	0.99
Prosthemium stellare	2.2	2.9	0.2	1.3	2.4	3.7	0.1	0.2	1.2	2.0	NS	1.68
Sarocladium strictum	0.3	2.0	4.0	4.8	1.7	1.6	4.3	2.0	2.6	2.6	NS	1.00

(B)	Bacteria	April		June		September		January		Mean	Mean	Statistics	Ratio
Family	Genus	Healthy	Disease	Healthy	Disease	Healthy	Disease	Healthy	Disease	Healthy	Disease	*P*-value	WR/NN
Acetobacteraceae	*Roseomonas* sp.	10.5	0.7	1.9	4.0	3.1	1.7	1.8	4.8	4.3	2.8	NS	0.65
Alcaligenaceae	nd	0.0	0.2	0.0	1.1	0.0	0.0	0.0	0.0	0.0	0.3	NS	nd
Bacillaceae	*Bacillus* sp.	0.7	0.7	0.5	0.5	5.4	2.9	1.8	0.0	2.1	1.0	NS	0.50
Bradyrhizobiaceae	nd	1.3	3.6	2.2	4.3	1.8	1.1	2.7	0.3	2.0	2.3	NS	1.17
Chitinophagaceae	nd	0.0	0.0	0.0	0.0	8.0	6.9	8.2	4.1	4.1	2.7	NS	0.68
Comamonadaceae	*Variovorax* sp.	1.3	4.6	6.1	20.1	4.9	4.0	8.2	9.6	5.1	9.6	NS	1.87
Cytophagaceae	*Spirosoma* sp.	2.0	18.6	1.0	1.9	2.7	6.3	2.7	2.4	2.1	7.3	NS	3.50
Enterobacteriaceae	***Pantoea* sp.**	**19.0**	**22.5**	**22.5**	**5.1**	**3.6**	**2.3**	**16.4**	**7.6**	**15.4**	**9.4**	**NS**	**0.61**
Geodermatophilaceae	*Modestobacter* sp.	9.2	5.1	1.7	13.9	10.7	15.4	7.3	12.0	7.2	11.6	NS	1.61
Hyphomicrobiaceae	*Devosia* sp.	0.7	0.5	2.7	0.5	0.9	1.7	0.9	2.1	1.3	1.2	NS	0.94
Moraxellaceae	*Acinetobacter* sp.	4.6	5.6	0.5	8.3	0.4	3.4	1.8	2.1	1.8	4.8	NS	2.64
Mycobacteriaceae	*Mycobacterium* sp.	3.3	4.6	5.3	1.3	3.6	3.4	10.0	4.5	5.5	3.5	0.048	0.62
Nocardioidaceae	nd	0.0	1.9	0.2	0.3	8.5	2.3	10.9	1.0	4.9	1.4	NS	0.28
Oxalobacteraceae	*Janthinobacterium* sp.	2.0	1.2	0.2	1.1	3.1	0.6	1.8	2.1	1.8	1.2	NS	0.69
Pseudomonadaceae	*Pseudomonas* sp.	1.3	0.0	1.5	0.3	0.4	1.1	0.0	0.0	0.8	0.4	NS	0.44
Rhizobiaceae	*Agrobacterium* sp.	7.8	5.6	19.9	9.4	4.9	8.0	2.7	19.6	8.8	10.6	NS	1.20
Sinobacteraceae	*Steroidobacter* sp.	3.3	1.0	0.5	1.1	1.3	5.7	2.7	4.5	2.0	3.1	NS	1.56
Sphingomonadaceae	***Sphingomonas* sp.**	**28.8**	**17.9**	**18.9**	**15.5**	**27.2**	**24.6**	**18.2**	**20.6**	**23.3**	**19.7**	**NS**	**0.84**
Trueperaceae	nd	2.6	1.9	12.8	0.8	8.9	2.9	0.9	0.7	6.3	1.6	NS	0.25
Xanthomonadaceae	*Stenotrophomonas* sp.	2.0	3.6	1.7	10.7	0.4	5.7	0.9	2.1	1.3	5.5	NS	4.41

% of reads for a single species, in bold values over 10%; NN: non necrotic woody tissues of cordon from infected plants; WR: white-rot necrotic woody tissues of cordon from infected plants; NS: non-significant, nd: not done.

Sphingomonadaceae included only two OTUs, corresponding to *Sphingomonas* spp. and *Kaistobacter* spp., respectively. *Cytophagaceae* also included only two OTUs, corresponding to *Pelomonas* spp. and *Spirosoma* spp., respectively. *Pantoea* spp. from *Enterobacteriaceae*, one of the most abundant genera in woody tissues (13%, Supporting Information Table S4), and *Bacillus* spp. (1.7%, Supporting Information Table S4) had antagonistic properties. Strains from these two genera, isolated from grapevine woody tissues inhibited the growth of fungi involved in GTDs (Haidar *et al*., 2016; Rezgui *et al*., 2016). Their presence in grapevine woody tissues may influence the development of GTD fungi, and their effectiveness as biological control agents merits further evaluation. Statistical analyses were performed for each bacterial species, using values from different sampling dates as biological replicates. In healthy plants, the relative abundance of OTUs from two families (*Geodermatophilaceae*, *Sphingomonadaceae*) differed between cordons and other organs (Supporting Information Tables S2 and S4). In diseased plants, the relative abundance of OTUs from four families (*Acetobacteraceae*, *Geodermatophilaceae*, *Oxalobacteraceae*, *Sphingomonadaceae*) significantly differed between organs (Supporting Information Table S2). Comparisons of bacterial microbiota between healthy and diseased plants were performed for each organ (Supporting Information Table S2), with an emphasis on cordon (Table 2B). In cordon, the relative abundance of a single OTU from *Mycobacteriaceae*, Mycobacterium spp., significantly differed between healthy and diseased plants (1.5-fold decrease in diseased plants (Table 2B and Supporting Information Table S2).

Variations in the taxonomic composition of bacterial and fungal microbiota between necrotic and non-necrotic woody tissues of cordon from diseased plants

The woody tissues of cordon from diseased plants were split into non-necrotic tissues and white-rot necrotic tissues. ANOSIM analyses showed that fungal taxonomic composition significantly differed between white-rot necrotic and surrounding non-necrotic tissues (P = 0.03, Fig. 3A). Fungal microbiota from white-rot necrotic tissues were dominated by the two species *F. mediterranea* (68%–97%, average 85%, Table 3A) and *P. chlamydospora* (2%–28%, average 13%, Table 3A). All other fungal species were detected at a low abundance (<0.5%). We did not identify fungal species specific of white-rot tissues (Table 3A). The dominance of fewer fungal species in white-rot necrotic tissues was mirrored by their low Shannon and Simpson index values (0.97 and 0.41, respectively, Table 1), compared to values from surrounding non-necrotic tissues (2.77 and 0.83, respectively, Table 1). The taxonomic diversity of fungal microbiota was more diverse in non-necrotic tissue (Tables 1 and 3A) than was the case in white-rot necrotic tissue. The most abundant species in non-necrotic tissues was *P. chlamydospora* (15%–51%, average 34%). It was associated with 14 other fungal species (>1%), including GTD fungi such as *F. mediterranea* (6.5%), *D. seriata* (6.6%) and *N. parvum* (2.5%). Comparisons of fungal microbiota between white-rot and non-necrotic tissue from diseased plant cordons were performed for each fungal species, using values from different sampling dates as biological replicates (Supporting Information Table S2). *F. mediterranea* was the only fungal species in which abundance significantly increased in white-rot necrotic tissues compared with the surrounding non-necrotic tissue (13-fold; Table 3A; Supporting Information Table S2). Seven fungal species from non-necrotic tissues were not identified in white-rot necrotic tissues (Table 3A). The relative abundance of seven other fungi strongly decreased in white-rot necrotic tissues (10- to 150-fold, Table 3A), even though significant differences were only detected for two of them, *Camarographorium koreanum* and *Microsphaeropsis arundinis* (Table 3A). Five fungal species showed similar relative abundances between white-rot and non-necrotic tissues including the

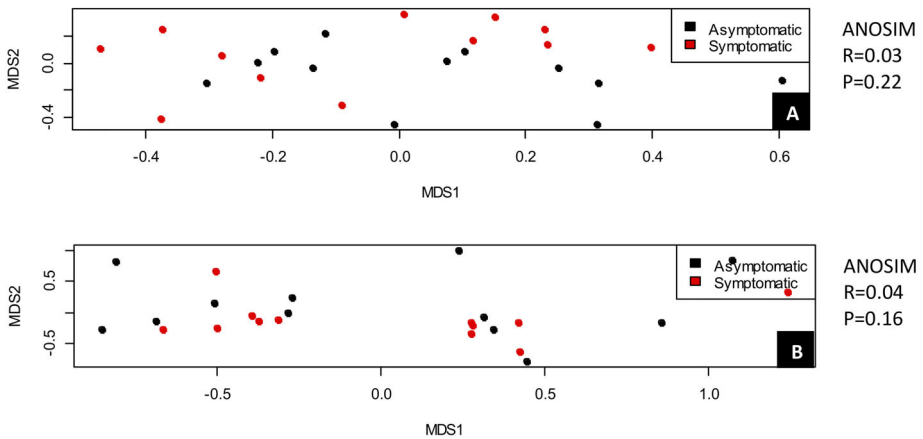

Fig 3. Non-metric multidimensional scaling (NMDS) analysis of fungal and bacterial communities based on Bray–Curtis dissimilarity. Data used for this analysis contain all OTUs. NMDS plot of fungal (A) and bacterial (B) communities from white-rot tissues of the cordon from healthy and diseased vines.

Table 3. Proportions (%) of the 20 most abundant species of fungi (A) and bacteria (B) in the white-rot and the non-necrotic tissues of the cordon of esca-foliar symptomatic vines.

(A) Fungi	April		June		September		January		Mean	Mean	Statistics	Ratio
Specie	NN	WR	NN	WR	NN	WR	NN	WR	NN	WR	*P*-value	WR/NN
Asterosporium betulinum	0.3	0.0	0.1	0.0	0.5	0.6	0.0	0.1	0.2	0.2	NS	0.76
Aureobasidium pullulans	1.1	0.1	1.0	0.0	3.4	0.0	1.2	0.0	1.7	0.0	nd	0.02
Bionectria ochroleuca	10.2	0.1	0.5	0.1	0.4	0.0	0.0	0.4	2.8	0.1	NS	0.05
Camarographium koreanum	45.7	0.2	2.7	0.0	3.5	0.1	0.5	0.0	13.1	0.1	NS	3.31
Cladosporium cladosporioides	0.9	0.0	1.0	0.0	2.1	0.0	2.4	0.0	1.6	0.0	nd	0.00
Diaporthe eres	6.5	0.1	18.4	0.1	7.0	0.1	2.6	0.0	8.6	0.1	0.001	0.01
Diplodia seriata	2.4	0.3	1.5	0.1	2.6	0.0	19.9	0.0	6.6	0.1	NS	0.02
Epicoccum nigrum	0.3	0.0	0.7	0.0	0.2	0.0	0.0	0.0	0.3	0.0	nd	0.00
Fomitiporia mediterranea	**5.3**	**92.6**	**13.2**	**81.8**	**4.3**	**68.4**	**3.3**	**97.1**	**6.5**	**85.0**	**0.001**	**13.05**
Lophiostoma cynaroidis	0.2	0.1	0.1	0.0	2.1	0.0	0.1	0.0	0.6	0.0	nd	0.02
Massarina rubi	0.3	0.1	0.4	0.0	0.8	0.2	0.1	0.0	0.4	0.1	NS	0.20
Microsphaeropsis arundinis	4.0	0.2	2.3	0,0	31.1	0.0	7.4	0.1	11.2	0.1	NS	0.01
Neofabraea malicorticis	0.4	0	2.0	0	0.4	0	5.9	0	2.2	0.0	nd	0.00
Neofusicoccum parvum	1.2	0.1	4.4	0.0	4.1	0.0	0.3	0.0	2.5	0.0	nd	0.01
Ochrocladosporium elatum	0.4	0.0	1.8	0.3	0.2	1.1	0.0	0.0	0.6	0.4	NS	0.57
Phaeoacremonium minimum	0.1	0.2	2.4	0.3	0.9	0.4	2.7	0.4	1.5	0.3	NS	0.22
Phaeomoniella chlamydospora	**15.3**	**5.4**	**39.4**	**17.1**	**29.6**	**28.6**	**50.9**	**1.8**	**33.8**	**13.2**	**NS**	**0.39**
Phialophora sessilis	0.4	3.3	1.9	3.3	1.4	0.0	0.4	0.0	1.0	0.1	0.35	0.09
Prosthemium stellare	2.9	0.4	1.3	0.0	3.8	0.3	0.2	0.0	2.0	0.2	NS	0.09
Sarocladium strictum	2.0	0.0	4.8	0.0	1.6	0.1	2.0	0.0	2.6	0.0	nd	0.01

(B)	Bacteria	April		June		September		January		Mean	Mean	Statistics	Ratio
Family	Genus	NN	WR	NN	WR	NN	WR	NN	WR	NN	WR	*P*-value	WR/NN
Acetobacteraceae	*Roseomonas* sp.	0.7	3.8	4.0	2.1	1.7	1.7	4.8	0.0	2.8	1.9	NS	0.68
Alcaligenaceae	nd	0.2	7.7	1.1	4.2	0.0	0.0	0.0	0.0	0.3	3.0	NS	9.04
Bacillaceae	*Bacillus* sp.	0.7	0.0	0.5	0.0	2.9	0.0	0.0	0.0	1.0	0.0	nd	0.00
Bradyrhizobiaceae	nd	3.6	0.0	4.3	8.3	1.1	5.6	0.3	14.3	2.3	7.1	NS	3.01
Chitinophagaceae	nd	0.0	0.0	0.0	0.0	6.9	13.0	4.1	2.9	2.7	4.0	NS	1.44
Comamonadaceae	*Variovorax* sp.	4.6	1.9	20.1	16.7	4.0	7.9	9.6	8.6	9.6	8.8	NS	0.92
Cytophagaceae	*Spirosoma* sp.	18.6	1.9	1.9	2.1	6.3	0.0	2.4	0.0	7.3	1.0	NS	0.14
Enterobacteriaceae	*Pantoea* sp.	22.5	0.0	5.1	0.0	2.3	0.0	7.6	0,0	9.4	0.0	nd	0.00
Geodermatophilaceae	***Modestobacter* sp.**	**5.1**	**1.9**	**13.9**	**10.4**	**15.4**	**4.0**	**12.0**	**8.6**	**11.6**	**6.2**	**0.03**	**0.54**
Hyphomicrobiaceae	*Devosia* sp.	0.5	3.8	0.5	0.0	1.7	1.1	2.1	0.0	1.2	1.2	NS	1.04
Moraxellaceae	*Acinetobacter* sp.	5.6	0.0	8.3	0.0	3.4	0.0	2.1	0.0	4.8	0.0	nd	0.00
Mycobacteriaceae	***Mycobacterium* sp.**	**4.5**	**23.1**	**1.3**	**14.6**	**3.4**	**5.1**	**4.5**	**22.9**	**3.5**	**16.4**	**NS**	**4.74**
Nocardioidaceae	nd	1.9	3.8	0.3	2.1	2.3	2.3	1.0	5.7	1.4	3.5	NS	2.52
Oxalobacteraceae	*Janthinobacterium* sp.	1.2	0.0	1.1	0.0	0.6	1.7	2.1	0.0	1.2	0.4	NS	0.34
Pseudomonadaceae	*Pseudomonas* sp.	0.0	0.0	0.3	0.0	1.1	0.0	0.0	0.0	0.4	0.0	nd	0.03
Rhizobiaceae	*Agrobacterium* sp.	5.6	1.9	9.4	6.3	8.0	12.4	19.6	2.9	10.6	5.9	NS	0.55
Sinobacteraceae	*Steroidobacter* sp.	1.0	0.0	1.1	0.0	5.7	0.0	4.5	2.9	3.1	0.7	0.03	0.23
Sphingomonadaceae	***Sphingomonas* sp.**	**17.9**	**50.0**	**15.5**	**33.3**	**24.6**	**38.4**	**20.6**	**28.6**	**19.7**	**37.6**	**NS**	**1.91**
Trueperaceae	nd	1.9	0.0	0.8	0.0	2.9	6.8	0.7	0.0	1.6	1.7	NS	1.08
Xanthomonadaceae	*Stenotrophomonas* sp.	3.6	0.0	10.7	0.0	5.7	0.0	2.1	2.9	5.5	0.7	0.003	0.13

Highest percentages are highlighted in bold. The data of non-necrotic tissues are the same as Table 2. % of reads for a single species, in bold, values over 10%; NN: non-necrotic woody tissues of cordon from infected plants; WR: white-rot necrotic woody tissues of cordon from infected plants; NS: non-significant, nd: not done.

GTD fungus *P. chlamydospora* (Table 3A). Overall, white-rot necrotic tissue was characterized by a simplified microbiota compared to non-necrotic tissue (−70% of species), corresponding mostly to the co-existence of the two fungal species, *P. chlamydospora* and *F. mediterranea*.

Bacterial microbiota from white-rot necrotic tissues were dominated by two OTUs, one from *Sphingomonadaceae* (37%) the other from *Mycobacteriaceae* (16%, Table 3B). These dominant OTUs were associated with two other major OTUs (>7%), respectively, from *Bradyrhizobiaceae* and *Comamonadaceae*. We did not identify bacterial OTUs specific of white-rot tissues. Bacterial microbiota from surrounding non-necrotic tissue were dominated by a single OTU from *Sphingomonadaceae* (24%), associated with four other major OTUs (>7%, Table 3B). All bacterial OTUs from white-rot necrotic tissues and surrounding non-necrotic tissues were identified at the genus level (Supporting Information Table S5). Four families included only two OTUs from different genera, as observed for *Sphingomonadaceae*, corresponding to *Kaistobacter* spp. and *Sphingomonas* spp. Other families corresponded to a single OTU from a specific genus, as observed for *Mycobacteriaceae* (*Mycobacterium* spp.) and Enterobacteriaceae (*Pantoea* spp.). ANOSIM analyses showed that the bacterial taxonomic composition significantly differed between white-rot necrotic and surrounding non-necrotic tissues ($P = 0.03$, Fig. 3B). Comparisons of bacterial microbiota from white-rot and non-necrotic tissues from diseased plant cordons were performed for each bacterial species, using values from different sampling dates as biological replicates (Table 3B; Supporting Information Table S2). *Mycobacterium* spp. displayed a higher relative abundance in white-rot necrotic tissues (4.5-fold) compared with non-necrotic tissues (Table 3B). However, this difference was not supported statistically (Supporting Information Table S2). Four other bacterial OTUs, including *Sphingomonas* spp., had a pattern similar to *Mycobacterium* spp. (increase in white-rot tissues not statistically supported). Four bacterial OTUs from non-necrotic tissues were not identified in white rot necrotic tissues (Table 3). The relative abundance of five bacterial OTUs detected in non-necrotic tissues strongly decreased in white-rot necrotic tissues (Table 3B). Significant differences were detected for three of them (*Modestobacter*, *Steroidobacter*, *Stenotrophomonas*, Supporting Information Table S2). Overall, bacterial microbiota from white-rot necrotic tissues were characterized by a simplified microbiota compared to non-necrotic tissues (−50% absent or reduced OTUs) corresponding mainly to the co-existence of two bacterial taxa, *Sphingomonas* spp. and *Mycobacterium* spp.

Visualization of fungi and bacteria inside grapevine woody tissues

Fungi and bacteria colonizing grapevine woody tissues were observed using cytological methods (Figs. 4–6 and S3 and S4). The plant selection (June and January) was based on our NMDS analysis, which highlighted differences in bacterial communities between June 2010 and January 2011 (Fig. 2C). Using WGA-Alexa staining, fungi were detected in all woody tissues of cordon and trunk from healthy and diseased plants sampled in June and January (Fig. 4). In non-necrotic woody tissue of cordon from both healthy and diseased plants, fungi were abundant in xylem vessels, in tissue surrounding fiber, and in parenchyma (Fig. 4). Fungi were also observed in white-rot necrotic tissue specific of cordon from diseased plants, despite technical difficulties in staining such highly decomposed tissues (data not shown). Using DOPE-FISH and a mixed EUB probe, we observed large numbers of bacteria in xylem, and their surrounding woody tissues of cordon (Fig. 5) and trunk (Figs. S2–S4) from both healthy and diseased plants from June and January. *Actinobacteria*, *Alphaproteobacteria*, *Gammaproteobacteria*, and *Firmicutes* were detected in all woody tissues from cordons and trunks (Fig. 5 and Supporting Information Figs. S2–S4). Only *Actinobacteria*, *Alphaproteobacteria* and *Gammaproteobacteria* were detected in abundance in non-necrotic cordon tissues (Fig. 5). According to these observations, *Proteobacteria* were the most abundant bacteria in non-necrotic woody tissue of cordon, while *Actinobacteria* dominated the non-necrotic woody tissue of trunks. These cytological observations are in agreement with our meta-barcoding data, showing that these bacterial taxa are the most abundant in their respective woody tissues (Tables 2B and 3B; Supporting Information Table S4). Visualization of bacteria in white-rot necrotic tissue from cordons of diseased plants highlighted mainly *Alphaproteobacteria*, *Gammaproteobacteria*, and Firmicutes (Fig. 6). *Sphingomonas* spp., one of the most abundant genera in white-rot necrotic tissues according to meta-barcoding (37%, Table 3B), belongs to *Alphaproteobacteria*. Since this genus corresponded to 18% of all the *Alphaproteobacteria* detected by meta-barcoding in these tissues (Table 3B), we suggest that the *Alphaproteobacteria* specific DOPE-FISH signal we have observed, mostly reflects the abundance of *Sphingomonas* spp. in these tissues. Overall, our cytological observations were in agreement with our meta-barcoding data, identifying *Proteobacteria* (*Alpha*-, *Gamma*-) and *Actinobacteria* as the most abundant bacterial taxa in grapevine woody tissues. In addition, these cytological observations strongly suggested that fungi and bacteria co-existed in the same woody tissues of trunks and cordons. We observed fungi

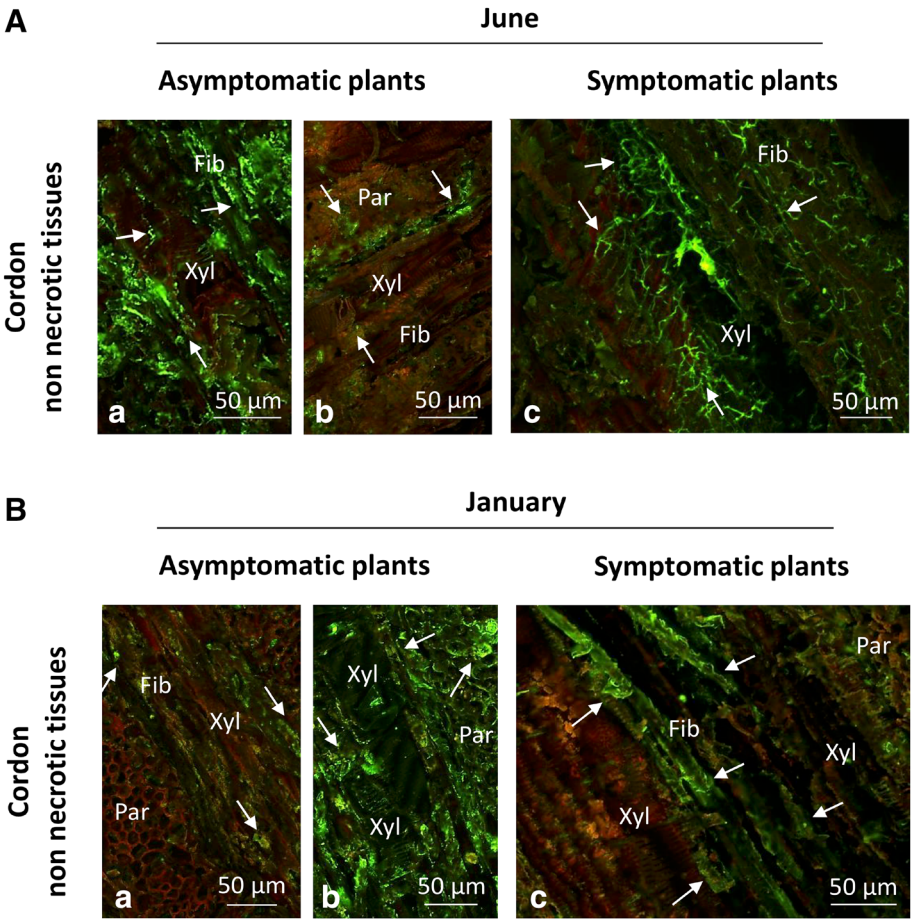

Fig 4. Detection of fungi in non-necrotic woody tissues of cordons from healthy (asymptomatic) and diseased (symptomatic) grapevines. Non-necrotic woody tissues from grapevine cordons were sampled in June 2010 (A) or January 2011 (B). Fungi were stained using WGA-Alexa Fluor488®. Fib = fiber, Xyl = xylem, Par = parenchyma.
A, a: Fungi detected in green in parenchyma of non-necrotic tissue asymptomatic grapevines sampled in June 2010.
A, b: Fungi detected in green in fiber and xylem of non-necrotic tissue asymptomatic grapevines sampled in June 2010.
A, c: Fungi detected in green in parenchyma, fiber and xylem of non-necrotic tissue symptomatic grapevines sampled in June 2010.
B, a: Fungi detected in green in xylem of non-necrotic tissue asymptomatic grapevines sampled in January 2011.
B, b: Fungi detected in green in parenchyma and fiber of non-necrotic tissue asymptomatic grapevines sampled in January 2011.
B, c: Fungi detected in green in parenchyma of non-necrotic tissue asymptomatic grapevines sampled in January 2011.

and bacteria in the same zones of woody tissues such as fiber, parenchyma and xylem vessels (Figs. 5A and 6B,C).

Discussion

This study identified variations in the taxonomical composition of fungal and bacterial communities colonizing grapevine woody tissues according to season, organ, and esca disease status. These communities were characterized using meta-barcoding, revealing 515 fungal and 403 bacterial OTUs. Only 20 fungal species and 50 bacterial genera, however, were detected in abundance greater than 1%, and most taxa were in very low abundance (<0.1%), as observed in other ecosystems (Buée *et al*., 2009; Zhang *et al*., 2012).

Fungal microbiota of non-necrotic woody tissues from young grapevines

Our meta-barcoding analysis revealed that *P. chlamydospora* is the most abundant fungal species in non-necrotic woody tissues from cordons and trunks of young grapevines (11%–60%, average: 30%; Table 2A; Supporting Information Table S3). However, only a few strains of *P. chlamydospora* were isolated from the same non-necrotic woody tissues using microbiological methods (10/1500 isolates: 0.6%; Bruez *et al*., 2014). Quantification of *P. chlamydospora* using qPCR confirmed its high abundance in our samples, suggesting that taxa quantification using meta-barcoding was reliable, as observed for microbiota on grapevine leaves (Gobbi *et al*., 2020). The discrepancy in fungal quantification between meta-barcoding and microbiological methods could result from the difficulty in isolating *P. chlamydospora* from the woody tissues studied. This fungal species is easily isolated in the black necrotic sectors of trunks from old diseased grapevines, which are almost exclusively colonized by this fungus (Bertsch *et al*., 2013; Mondello *et al*., 2018). The fungal microbiota of non-necrotic woody tissues was more complex, and contained fungal species with very different growth behaviour, including fast growing species such as *D. seriata* and *N. parvum*, and slow growing species such as *P. chlamydospora* (Supporting Information Table S3). For example, *D. seriata* and *N. parvum* were isolated at a high frequency from trunks using microbiological methods (322/1500 isolates: 21%; Bruez *et al*., 2014), despite their lower relative abundance according to meta-barcoding

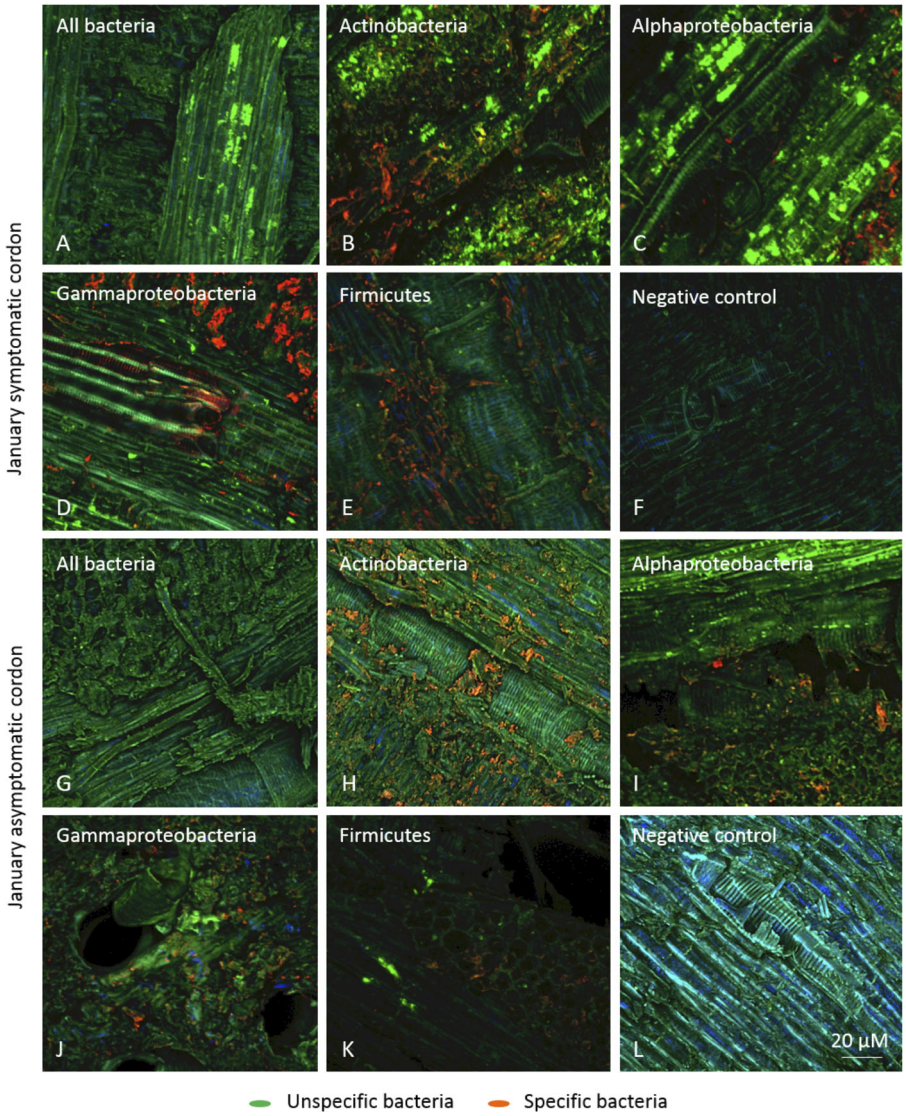

Fig 5. Detection of bacterial taxa in non-necrotic woody tissues of cordons from healthy (asymptomatic) and diseased (symptomatic) grapevines using DOPE-FISH/CLSM. Non-necrotic woody tissues from cordons were sampled in January 2011 from either diseased (symptomatic: A–F) or healthy (asymptomatic: G–L) grapevines. Orange/reddish dots = positive detection of specific bacterial taxa from, Actinobacteria (B, H), Alpha-proteobacteria (C, I), Gamma-Proteobacteria (D, J) or Firmicutes (E, K). Negative control (F, L). Green dots = non-specific detection of all bacterial taxa.

(8%; Supporting Information Table S3). This comparison suggests that microbiological methods suffer from a competition between fast and slow growing fungi, which could reduce the recovery of *P. chlamydospora* from non-necrotic woody tissues. Other meta-barcoding studies were performed to characterize the fungal microbiota occurring on the surface of grapevine leaves and berries. Pinto *et al*. (2014) and Gobbi *et al*. (2020) identified a few abundant fungal taxa on the surface of grapevine leaves such as *Alternaria* spp., *A. pullulans*, *Cladosporium* spp., *Sporobolomyces spp*. and species from *Pleosporalaceae*. Except for *A. pullulans* and *Cladosporium* spp., these fungal species from leaves were not identified in young grapevine woody tissues (Supporting Information Table S3). Bokulich *et al*. (2013) identified, mostly on grape berries, *Cladosporium* spp., *Botryotinia fuckeliana* (*Botrytis cinerea*), *Penicillium* spp., *Davidiella tassiana*, and *A. pullulans*. Except for *A. pullulans* and *Cladosporium* spp., these fungal species from berries were not identified in young grapevine woody tissues (Supporting Information Table S3). Overall, only 3 abundant taxa (>1%) out of 20 were shared between these studies and our analysis (15%), indicating that fungal microbiota from inner wood strongly differs from those of berry and leaf surface.

Bacterial microbiota of non-necrotic woody tissues from young grapevines

Our meta-barcoding analysis revealed a few abundant bacterial taxa in non-necrotic woody tissues, corresponding to *Pantoea* spp., *Bacillus* spp., *Enterobacter* spp., *Paenibacillus* spp. and *Stenotrophomonas* spp. (>10%, Supporting Information Table S4). In the work of

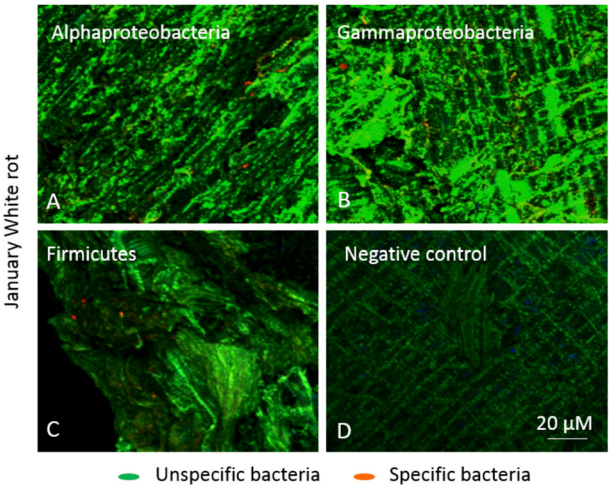

Fig 6. Detection of bacterial taxa in white-rot necrotic woody tissues of cordons from diseased (Symptomatic) grapevines using DOPE-FISH/CLSM. White-rot necrotic woody tissues from cordons were sampled in January 2011 from diseased grapevines (A-D). Orange/reddish dots = positive detection of bacterial taxa from Alpha-proteobacteria (A), Gamma-Proteobacteria (B), or Firmicutes (C). Negative control (D). Green dots = non-specific detection of all bacterial taxa.

Niem *et al*. (2020), meta-barcoding analysis of bacterial microbiota from woody tissues was performed, using old grapevines from Australia that displayed BDA, but not esca disease. In trunks from healthy plants, these authors identified mostly *Pseudomonas* (50%–75%), *Roseococcus* (16%) and *Chitinophagaceae* (13%). In our study, *Pseudomonas* and *Chitinophagaceae* were detected in the non-necrotic woody tissue of trunks from healthy plants, but at a much lower abundance (1.4% and 1.7%, respectively, Supporting Information Table S4). These quantitative differences were also observed for *Sphingomonas* spp., detected at a lower abundance in woody tissues of Australian grapevines (6%) than those of French grapevines (17%, Table S4). In these studies, 7 abundant taxa (>1%) out of 20 were identified to a total of 35%. These differences could result from variations in ecological factors affecting microbial colonization between these two vineyards (location, cultivar, age, cultural practices). We also compared our data with those obtained using microbiological isolation methods and the same young grapevines (Bruez *et al*., 2015). This study identified *Pantoea* spp., *Bacillus* spp., *Enterobacter* spp., *Paenibacillus* spp. and *Stenotrophomonas* spp. as the main bacterial genera, which were also identified as abundant by meta-barcoding. However, *Sphingomonas* spp., the most abundant bacterial taxa according to meta-barcoding (average 18%, Supporting Information Table S4), was only poorly recovered by microbiological methods (<2%; Bruez *et al*., 2015). This comparison showed that both methods have a similar efficiency in detecting most of the main bacteria colonizing woody tissues. Other meta-barcoding studies were performed to characterize the bacterial microbiota occurring on the surface of grapevine berries, flowers, leaves and roots (Compant *et al*., 2011, Bokulich *et al*., 2013; Gilbert *et al*., 2014; Zarraonaindia *et al*., 2015; Gobbi *et al*., 2020). These studies identified *Pseudomonas* spp. as the most abundant genus on the surface of flowers and leaves, while berry bacterial microbiota was predominantly composed of OTUs from *Erwinia* spp., *Klebsiella* spp., *Lactococcus* spp., *Pseudomonas* spp., *Sphingomonas* spp., and *Methylobacterium* spp. Overall, only 2 abundant taxa (>1%, *Sphingomonas* spp., *Pseudomonas* spp., Supporting Information Table S4) out of 20 were shared between these studies and our analysis (10%). These comparisons showed that bacterial taxa colonizing inner wood strongly differ from those occurring at the surface of grapevine.

Fungal and bacterial microbiota of white-rot necrotic tissues, a hallmark of cordons from diseased grapevines

Most cordons from diseased plants (70%) displayed white-rot necrotic tissues colonized by only a few plant pathogenic fungi (*F. mediterranea* and *P. chlamydospora*) and bacterial taxa (*Sphingomonas* spp. and *Mycobacterium* spp.). Since these fungal and bacterial taxa are known to degrade plant cell walls, their association could be essential for the degradation of inner wood and the formation of white-rot necrotic tissues. The presence of white-rot necrotic tissues is strongly associated with esca disease (70% of diseased grapevines, absence in healthy grapevines). However, these tissues were not detected in the trunks of these diseased grapevines. To account for this observation, we suggest that *F. mediterranea* was recently infected cordons of these young grapevines through pruning wounds. We propose that the development of *F. mediterranea* in these cordons could ultimately lead to the formation of the observed central white-rot necrosis. This colonization has not reached yet trunks that are devoid of white-rot necrosis. Such entry and development of *F. mediterranea* in woody tissues has been observed after citrus pruning (Kalomira *et al*. 2006), but not yet for grapevine. Consequently, we propose a scenario for the involvement of this white-rot specific microbiota in the onset of esca disease. First, we propose that *F. mediterranea* infects cordon from young grapevine via pruning wounds. It then progresses in cordon woody tissue already colonized by *P. chlamydospora*. The interaction between *P. chlamydospora*, *F. mediterranea* and bacteria found in these tissues is probably essential for the formation of white-rot necrotic tissue in the cordon of young grapevines. We also propose that *F. mediterranea* and its associated microbiota will over time progress from cordon

to trunk. This would allow the formation of white-rot necrotic tissues in trunks, as observed in old grapevines with esca-disease (Maher *et al*., 2012; Bertsch *et al*., 2013; Bruez *et al*., 2014; Bruez *et al*., 2015; Mondello *et al*., 2018; Elena *et al*., 2018; Del Frari *et al*., 2019; Nerva *et al*., 2019). Finally, we propose that this white-rot associated microbiota is essential for the onset of esca disease. In particular, the interaction between *F. mediterranea*, *P. chlamydospora* and bacteria from white-rot necrotic tissues could induce the production of novel phytotoxic secondary metabolites, thereby giving rise to typical esca-foliar symptoms. This production of novel fungal secondary metabolites by co-culture with bacteria is now well-documented *in vitro* (Haidar *et al*., 2016), and this phenomenon could happen *in natura*. This hypothesis needs to be supported by experiments, such as inoculating a mixture of fungal and bacterial species to pruning wounds of cordons, followed by the assessment of white-rot necrotic tissues, and esca symptom development over multiple years. Such experiments have already been performed with young grapevines (7–9 years old; Surico *et al*., 2008) with some success. Various mixtures of *F. mediterranea* and *P. chlamydospora* were able to induce the formation of white-rot necrotic tissues and esca leaf symptoms over 3 years of survey (Surico *et al*., 2008). Novel mixed inoculations were recently performed with *P. chlamydospora* and either *F. polymorpha* or *T. texanus*, two Basidiomycota colonizing white-rot necrotic tissues of US grapevines (Brown *et al*., 2020). These mixed inoculations induced large brown lesions of woody tissues not observed when inoculating a single species, and leaf lesions typical of esca, although at a low frequency. These experiments suggest a synergy between these fungi during the onset of esca. Additional mixed inoculations of fungal species (with wood inhabiting bacteria or not) should performed with different grapevines to validate these first results. For example, *F. mediterranea* could also be inoculated to grapevines already colonized by *P. chlamydospora*. Finally, *in vitro* co-cultures of *F. mediterranea* and *P. chlamydospora* (with or without bacteria) could be used to monitor the production of novel secondary metabolites toxic to grapevine. One possible reservation against generalizing our hypothesis to other vineyards is that *Basidiomycota* other than *F. mediterranea* are colonizing the trunk of from diseased grapevines in vineyards from other countries such as South/North America (*Fomitiporia polymorpha* and *T. texanus*: NorthAmerica; *Inocutis jamaicensis* and *Fomitiporella vitis*: SouthAmerica; Fisher, 2006; Brown *et al*., 2020) and South Africa (*Fomitiporia capensis*, *Cloete et al*., 2014). However, it is still possible that white-rot necrotic tissues from such grapevines are colonized by a few fungal taxa, including a major wood-degrading species other than *F. mediterranea*. Meta-barcoding analyses of cordon microbiota from other young and old grapevines are needed to generalize our finding (see below).

Comparison of fungal microbiota of woody tissues from young grapevines to those reported for old grapevines

Two other meta-barcoding studies of fungal microbiota from woody tissues were performed, using old grapevines from Portugal (Del Frari *et al*., 2019), or Australia (Niem *et al*., 2020). These authors studied old grapevines that were either healthy or displaying esca (Portugal) or BDA (Australia). The methods used for sampling the wood differed from ours. In Portugal, trunks and arms/cordons were drilled with a gimlet to avoid plant destruction. This method, however, does not allow easy characterization of the type and amount of internal necroses, or enable the split between non-necrotic and necrotic tissues to be split for microbiota analysis. In Australia, woody tissues from trunks were dissected, but necrotic and non-necrotic tissues were not split. Because of their sampling strategies, these authors could not identify which microbiota was colonizing necrotic tissues in diseased plants. Still, we nonetheless their results can be compared to our data for healthy plants. Both authors showed that *P. chlamydospora* was the most abundant fungal species in woody tissues from healthy old grapevines (50% in Portugal; 80% in Australia), as observed in France (41%, Supporting Information Table S3). In Portugal, *P. chlamydospora* was also the most abundant fungal species in woody tissues of cordons/arms from healthy grapevines (40%), as observed in France (48%, Supporting Information Table S3). The abundance of *P. chlamydospora* in grapevine woody tissues was unexpected, but the Portuguese results strongly suggest that this fungal species is one of the main colonizers of grapevine woody tissue. Grapevines displaying esca-foliar symptoms for at least 4 years have only been studied in Portugal. The authors showed that *P. chlamydospora* was less abundant in woody tissues from trunks of diseased plants (21%, twofold reduction) compared to healthy plants. The only fungal species in which relative abundance increased in trunks and arms/cordons of diseased compared to healthy plants was *F. mediterranea* (fivefold, up to 35%). The authors also stated that whereas they observed white-rot necrotic tissues only in diseased plants, this was limited to in 15% of their drilling samples. These observations suggest that esca disease is associated with the development of white-rot necrosis in woody tissues that are probably dominated by *F. mediterranea* in both cordon and trunk in old grapevines, thereby supporting our hypothesis which is based on observations of young grapevines.

Conclusion

Accurately determining the microbiota of grapevine woody tissues, using meta-barcoding, is crucial in understanding esca disease. Our statistical analyses showed that fungal microbiota from non-necrotic woody tissues from healthy or diseased grapevines, did not significantly differ (Supporting Information Table S2). We also showed that *P. chlamydospora* is the main fungal species colonizing woody tissues of grapevines. In healthy grapevines, its high incidence did not cause either visible local necrosis, or esca symptoms, suggesting a possible non-pathogenic endophytic behaviour. Our results support previous findings that *P. chlamydospora* could switch from an endophytic to a pathogenic lifestyle in response to biotic and abiotic factors (Bertelli *et al*., 1998; Pierron *et al*., 2016). The only difference that we found between healthy and diseased young grapevines was the presence of white-rot necrotic tissue in cordon. This typical necrotic tissue was dominated by *F. mediterranea*, associated with *P. chlamydospora*, and a few bacterial taxa (Table 3). Our hypothesis is that this microbial association is essential for the development of white-rot necrosis in the inner wood of cordon and is associated with the onset of esca. In future work, it will be important to study the microbiota of grapevine wood in other vineyards with esca disease by splitting non-necrotic and necrotic tissues, in order to survey the presence of white-rot necrotic tissue and decipher its associated microbiota in relation to the onset of esca disease. Other meta-barcoding studies in Portugal (Del Frari *et al*., 2019) suggest that our observations on young grapevines could be extended to old grapevines, since its authors identified only white-rot necrotic tissue in the trunk of diseased plants and confirmed the high abundance of *F. mediterranea* in trunk and cordon of these diseased plants.

Experimental procedures

Study site and sampling collection

The experimentation was carried out on 10-year-old Cabernet Sauvignon grapevines (*Vitis vinifera* L.) grafted on the rootstock 101-14 Mgt, and planted in a sandy-clay soil. The sampling site was located at the Luchey-Halde vineyard in Pessac Léognan (Bordeaux, France). This vineyard has been inspected annually for esca-foliar symptoms ever since its plantation in 2000. Plants were defined as diseased (symptomatic) if they had previously expressed esca-foliar symptoms at least twice over the last 4 years (2005–2009) before sampling (2010). Plants were defined as healthy (asymptomatic) if they had not displayed any esca-foliar symptoms since 2000. Four healthy and four diseased grapevines were uprooted every 12 weeks during a 1-year period. Sampling was performed at four stages of grapevine development: April 2010 (bud break), June 2010 (flowering), September 2010 (harvest), and January 2011 (pruning). This sampling method was destructive, as plants were first uprooted before their organs, *i.e*., cordon, trunk and rootstock, were cut longitudinally, in order to verify their necrotic or healthy wood status. Non-necrotic tissues were sampled in both healthy and diseased plants, while white-rot necrosis, which is associated with esca, was sampled only in diseased plants. A total of 112 wood samples was therefore collected, corresponding to the non-necrotic tissues of 3 organs (rootstock, trunk, cordon) × 4 dates × 8 grapevines (4 esca-foliar symptomatic and 4 asymptomatic grapevines), plus 16 additional samples of white-rot (4 dates × 4 asymptomatic grapevines).

DNA extraction and tag-encoded 454 pyrosequencing

DNA extraction. For each grapevine collected in 2010 and 2011, 10 g of non-necrotic and white-rot (only diseased plants) tissues were sampled from cordons, trunks, and rootstocks. All samples were ground in liquid nitrogen with a one-ball mill of Dangoumau type, and kept at −80°C, prior to DNA extraction. DNA was extracted from 60-mg aliquots of woody tissues using the Indvisorb Spin Plant mini Kit (Eurobio, France), according to the manufacturer's instructions. DNA extracts were then quantified with a nanodrop (ND-1000; Nano-Drop Technologies, Wilmington, USA), and homogenized at a concentration of 10 ng.μl^{-1}. Based on previous fingerprinting analyses which showed no significant microbial differences between replicates (Bruez *et al*., 2014), DNA samples were then pooled (four DNAs from four independent dissected grapevines) at equimolar concentrations to obtain 28 samples to be analysed, corresponding to [4 dates × 2 disease status × 3 organs] + 4 samples of white-rot (sampled only in cordons of symptomatic grapevines).

The composition of grapevine wood microbial communities was characterized by tag-encoded 454 pyrosequencing. In the case of fungi, the pair of primers, ITS1 and ITS4F (White *et al*., 1990), was used to amplify the ITS1 and ITS2 regions of the nuclear ribosomal repeat unit. For bacteria, PCR amplifications targeted the V5-V6 variable region of the 16S rDNA gene. The pair of primers, 799f and 1115r (Redford *et al*., 2010), were chosen, as they do not amplify chloroplastic DNA. DNA was amplified by PCR in an Applied Biosystem 9700 (Applied Biosystem) in a reaction mixture (50 μl final volume) consisting of 2.5 U of Taq polymerase (GoTaqFlexi, Promega), 1X buffer, 1.5 mM $MgCl_2$, 200 μM of each dNTP, 0.5 μM of each tagged-primer and 60 ng of DNA. The cycling parameters were as follows: enzyme activation at 95°C for 5 min; 28 cycles of denaturation at 95°C

for 30 s, 55°C (fungi)/54°C (bacteria) for 30 s, 72°C for 1 min 15 s (fungi)/45 s (bacteria); and a final extension at 72°C for 5 min.

PCR products were then purified using the QIAquick PCR purification kit (Qiagen), and quantified using the Quant-iT™ PicoGreen® dsDNA Assay Kit (Invitrogen, Saint Aubin, France) on a ABI Prism 7900HT (Life Technologies-Invitrogen-A-BIOSYSTEM, Villebon-sur-Yvette, France). Libraries were then prepared at equimolar concentrations, i.e. 500 ng of DNA and sequenced using a Roche GS FLX+ 454 pyrosequencer (454 Life Sciences – Roche Company, Branford, CT) at the GeT-PlaGe sequencing service (Genome and Transcriptome Laboratory, Toulouse, France).

Post-run analysis

Fungal and bacterial data were processed as similarly as possible, using the Quantitative Insights Into Microbial Ecology (QIIME) pipeline (version 1.7.0) (Caporaso *et al*., 2010). In brief, sequences were selected according to the following initial criteria: (i) ≥450 nucleotides in length; (ii) a perfect match to the primers and the barcodes; and (iii) no ambiguous base allowed. Although the bacterial primers were designed to amplify bacterial DNA, we verified, using the software Metaxa, that, after denoising, no sequences of chloroplastic or mitochondrial origin were present in the bacterial dataset (Bengtsson *et al*., 2011). The V-Xtractor (Hartmann *et al*., 2010) and FungalITSextractor softwares were then used, respectively, to extract the V5-V6 region of the bacterial 16S rDNA gene and the fungal ITS1 and ITS2 regions. Microbial sequences were then binned into OTUs, using a 97% identity threshold with the UPARSE algorithm implemented in the USEARCH pipeline (Edgar, 2013), with the most abundant sequence from each OTU being selected as a representative sequence for that OTU. Taxonomy was assigned to OTUs, using the Basic Local Alignment Search Tool (BLAST) (Altschul *et al*., 1990) for each representative sequence against the GreenGenes reference database for bacteria (99% similarity), and the Fungal ITS Database produced by Nilsson and co-workers (Nilsson *et al*., 2010) (97% similarity).

Statistical analysis

All the statistical analyses were carried out using the R statistical software, version 3.1.1. OTU-distribution matrixes were used to perform rarefaction analyses and to calculate diversity (Shannon and Simpson) indexes with the EstimateS software package (Colwell, 2005). To compare different indexes between samples, an analysis of variance and a Kruskal–Wallis test were performed. Using the Vegan package, non-metric multidimensional scaling (NMDS) was performed based on Bray–Curtis dissimilarity and validated with an ANOSIM test.

DOPE-FISH/CSLM microscopy

Bacterial DOPE-FISH. DOPE-FISH microscopy was carried out to visualize bacterial taxa within plant tissues. Wood tissues were stored at −20°C after sampling. The samples were obtained from non-necrotic cordon and trunk tissue from healthy and diseased plants sampled in June or January. Only the white-rot necrotic tissues from diseased plants sampled in January were analysed. Fixation was carried out overnight at 4°C, in a paraformaldehyde solution (4% w/v in PBS 7.2) in Eppendorf tubes, and rinsed three times with PBS. Samples were then treated with a lysozyme solution (1 mg ml^{-1} in PBS) for 10 min at 37°C, followed by dehydration in an ethanol series (25%, 50%, 75%, and 99.9%; 15 min each step). DOPE-FISH was performed after cutting samples into small pieces, and then using probes from Eurofins (Germany) labelled at both 5′ and 3′ positions. A mixEUB (equivalent mixture of EUB338, EUB338II, EUB338III coupled with an ATTO488 fluorochrome), an ALF1B probe specific of Alphaproteobacteria, some Deltaproteobacteria and Spirochetes, a Gam42a probe specific of Gammaproteobacteria, a LGC probe specific of Firmicutes, and a HGC69A probe specific of Actinobacteria, all coupled to Cy5, were used. A NON-EUB probe, coupled with ATTO488 and Cy5, was also used independently as a negative control (Wallner *et al*., 1993; Daims *et al*., 1999). Hybridization was performed at 46°C, during 2 h 30 min, with 10–20 μl hybridization solution applied to each plant sample, placed on slides in a 50ml moist chamber (also housing a piece of tissue imbibed with 5 ml hybridization buffer). Each hybridization solution contained 20 mM Tris–HCl pH 8.0, 0.01% w/v SDS, 0.9 M NaCl, formamide at the concentration adapted for each probe: 15 ng μl^{-1} for a general probe, and 10 ng μl^{-1} for a specific probe. Post-hybridization was performed in 20 μl at 48°C for 30 min with a post-FISH pre-warmed solution containing 20 mM Tris–HCl pH 8.0, 0.01% (w/v) SDS, 5 mM EDTA pH 8.0 and NaCl at a concentration corresponding to the formamide concentration used. Samples were rinsed with distilled water before air-drying in the dark.

Fungal visualization. Plant sections used for bacterial observations were also used for fungal visualization. DOPE-FISH was not used for fungi, but fungal detection was performed instead using wheat germ agglutinin (WGA) coupled with an Alexa fluor488 fluorochrome. Samples were immersed in 1 ml of phosphate buffer saline (PBS, pH 7.2) containing 50 μg ml^{-1} of wheat germ agglutinin (WGA)-AlexaFluor®488 conjugate (Life

Technologies, USA), and incubated 2 h at 37°C, before rinsing twice with PBS.

Image analysis. For microscopic examination, samples on slides were observed under a confocal microscope (Olympus Fluoview FV1000 with multiline laser FV5-LAMAR-2 and HeNe(G)laser FV10-LAHEG230-2). X, Y, Z pictures of samples were taken at 405, 488, 633 nm using 10× and 20× objectives, observed with Imaris software and merged (RGB) using ImageJ software. Z Project Stacks were used to create figures. Pictures were cropped, and sharpened. All experiments were repeated at least eight independent times, using samples from three different plants.

Acknowledgements

This work received grants from Bordeaux Sciences Agro, the Regional Council of Aquitaine, the Jean Poupelain Foundation, the French Ministry of Agriculture, Food-processing Industry and Forest (programme CASDAR V90), and INRA SPE department. The authors would like to thank the Industrial Chair GTDfree (French National Research Agency and Jas Hennessy & Co) and also Pierre Darriet for the sampling of the plants at the Chateau Luchey-Halde, and Sylvie Bastien for her extremely helpful technical assistance. The authors would like to acknowledge Cost Action FA1303 for its support.

References

Altschul, S.F., Gish, W., Miller, W., Myers, E.W., and Lipman, D.J. (1990) Basic local alignment search tool. *J Molecul Biol* **215**: 403–410.

Bengtsson, J., Eriksson, K.M., Hartmann, M., Wang, Z., Shenoy, B.D., Grelet, G.A., *et al*. (2011) Metaxa: a software tool for automated detection and discrimination among ribosomal small subunit (12S/16S/18S) sequences of archaea bacteria eukaryotes mitochondria and chloroplasts in metagenomes and environmental sequencing datasets. *Antonie Van Leeuwenhoek* **100**: 471–475.

Bertelli, E., Mugnai, L., & Surico, G. (1998). Presence of Phaeoacremonium chlamydosporum in apparently rooted grapevine cuttings. *Phytopathologia mediterranea*, **37**, 79–82.

Bertsch, C., Ramírez-Suero, M., Magnin-Robert, M., Larignon, P., Chong, J., Abou-Mansour, E., *et al*. (2013) Grapevine trunk diseases: complex and still poorly understood. *Plant Pathol* **62**: 243–265.

Bokulich, N.A., Subramanian, S., Faith, J.J., Gevers, D., Gordon, J.I., Knight, R., *et al*. (2013) Quality-filtering vastly improves diversity estimates from Illumina amplicon sequencing. *Nat Methods* **10**: 57–59.

Brown, A.A., Lawrence, D.P., and Baumgartner, K. (2020) Role of basidiomycete fungi in the grapevine trunk disease esca. *Plant Pathol* **69**: 205–220.

Bruez, E., Vallance, J., Gerbore, J., Lecomte, P., Da Costa, J.-P., Guerin-Dubrana, L., *et al*. (2014) Analyses of the temporal dynamics of fungal communities colonizing the healthy wood tissues of esca leaf-symptomatic and asymptomatic vines. *PLoS ONE* **9**: e95928.

Bruez, E., Haidar, R., Alou, M.T., Vallance, J., Bertsch, C., Mazet, F., *et al*. (2015) Bacteria in a wood fungal disease: characterization of bacterial communities in wood tissues of esca foliar symptomatic and asymptomatic grapevines. *Front Microbiol* **6**: 1–12.

Buée, M., Reich, M., Murat, C., Morin, E., Nilsson, R.H., Uroz, S., and Martin, F. (2009) 454 pyrosequencing analyses of forest soils reveal an unexpectedly high fungal diversity. *New Phytol* **184**: 449–456.

Buttigieg, P.L., and Ramette, A. (2014) A guide to statistical analysis in microbial ecology: a community-focused living review of multivariate data analyses. *FEMS Microbiol Ecol* **90**: 543–550.

Calzarano, F., Di Marco, S., and Cesari, A. (2004) Benefit of fungicide treatment after trunk renewal of vines with different types of esca necrosis. *Phytopathol Mediterr* **43**: 116–124.

Caporaso, J.G., Kuczynski, J., Stombaugh, J., Bittinger, K., Bushman, F.D., Costello, E.K., *et al*. (2010) QIIME allows analysis of high-throughput community sequencing data. *Nature Met* **7**: 335–336.

Cloete, M., Fisher, M., Mostert, L., and Halleen, F. (2014) A novel *Fomitiporia* species associated with esca on grapevine in South African. *Mycol Progr* **13**: 303–311.

Colwell, R.K. (2005) EstimateS: statistical estimation of species richness and shared species from samples. Version 8 purloclcorg/estimates.

Compant, S., Mitter, B., Colli-Mull, J.G., Gangl, H., and Sessitsch, A. (2011) Endophytes of grapevine flowers, berries, and seeds: identification of cultivable bacteria, comparison with other plant parts, and visualization of niches of colonization. *Microbio Ecol* **62**: 188–197.

Cuadros-Orellana, S., Leite, L.R., Smith, A., Medeiros, J.D., Badotti, F., Fonseca, P.L., *et al*. (2013) Assessment of fungal diversity in the environment using metagenomics: a decade in review. *Fungal Genom Biol* **3**: 1–13.

Daims, H., Brühl, A., Amann, R., Schleifer, K.H., and Wagner, M. (1999) The Domain-specific probe EUB338 is insufficient for the detection of all bacteria: development and evaluation of a more comprehensive probe set. *Sys Appl Microbiol* **22**: 434–444.

Del Frari, G., Gobbi, A., Aggerbeck, M.R., Oliveira, H., Hansen, L.H., and Ferreira, R.B. (2019) Characterization of the wood mycobiome of *Vitis vinifera* in a vineyard affected by Esca. Spatial distribution of fungal communities and their putative relation with leaf symptoms. *Front Plant Sci* **10**: 910.

Edgar, R.C. (2013) UPARSE: highly accurate OTU sequences from microbial amplicon reads. *Nature Meth* **10**: 996–998.

Elena, G., Bruez, E., Rey, P., and Luque, J. (2018) Microbiota of grapevine woody tissues with or without esca-foliar symptoms in northeast Spain. *Phytopathol Mediterr* **57**: 425–438.

Fischer, M. (2006) Biodiversity and geographic distribution of basidiomycetes causing esca-associated white rot in grapevine: a worldwide perspective. *Phytopathol Mediterr* **45**: S30–S42.

de Freitas Sia, E., Marcon, J., Luvizotto, D.M., Quecine, M. C., Tsui, S., Pereira, J.O., *et al*. (2013) Endophytic fungi

from the Amazonian plant *Paullinia cupana* and from *Olea europaea* isolated using cassava as an alternative starch media source. *Springerplus* **2**: 579.

Gilbert, J.A., van der Lelie, D., and Zarraonaindaia, I. (2014) Microbial terroir for wine grapes. *PNAS* **11**: 6–7.

Gobbi, A., Kyrkou, I., Filippi, E., Ellegaard-Jensen, L., and Hansen, L.H. (2020) Seasonal epiphytic microbial dynamics on grapevine leaves under biocontrol and copper fungicide treatments. *Sci Rep* **10**: 681.

Haidar, R., Roudet, J., Bonnard, O., Dufour, M.C., Corio-Costet, M.F., Ferta, M., *et al*. (2016) Screening and modes of action of antagonistic bacteria to control the fungal pathogen *Phaeomoniella chlamydospora* involved in grapevine trunk diseases. *Microbiol Res* **192**: 172–184.

Hartmann, M., Howes, C.G., Abarenkov, K., Mohn, W.W., and Nilsson, R.H. (2010) V-Xtractor: an open-source high-throughut software tool to identify and extract hypervariable regions of small subunit (16S/18S) ribosomal RNA gene sequences. *J Microbiol Meth* **83**: 250–253.

Kalomira, E., Fischer, M., Dimou, D., and Dimou, D.M. (2006) *Fomitiporia mediterranea* infecting citrus trees in Greece. *Phytopathol Mediter* **45**: 35–39.

Lecomte, P., Darrieutort, G., Liminana, J.M., Comont, G., Muruamendiaraz, A., Legorburu, F.J., *et al*. (2012) New insights into Esca of grapevine: the development of foliar symptoms and their association with xylem discoloration. *Plant Disease* **96**: 924–934.

Niem, J.M., Billones-Baaijens, R., Stodart, B., and Savocchia, S. (2020) Diversity profiling of grapevine microbial endosphere and antagonistic potential of endophytic Pseudomonas against grapevine trunk diseases. *Front Microbiol* **11**: 477.

Nilsson, R.H., Veldre, V., Hartmann, M., Unterseher, M., Amend, A., Bergsten, J., *et al*. (2010) An open source software package for automated extraction of ITS1 and ITS2 from fungal ITS sequences for use in high-throughput community assays and molecular ecology. *Fungal Ecol* **3**: 284–287.

Nerva, L., Turina, M., Zanzotto, A., Gardiman, M., Gaiotti, F., Gambino, G., and Chitarra, W. (2019) Isolation, molecular characterization and virome analysis of culturable wood fungal endophytes in esca symptomatic and asymptomatic grapevine plants. *Environ Microbiol* **21**: 2886–2904.

Maher, N., Piot, J., Bastien, S., Vallance, J., Rey, P., and Guerin-Dubrana, L. (2012) Wood necrosis in Esca-affected vines: type relationships and possible links with foliar symptom expression. *J Int Sci Vigne et Vin* **46**: 15–27.

Mondello, V., Songy, A., Battiston, E., Pinto, C., Coppin, C., Trotel-Aziz, P., *et al*. (2018) Grapevine trunk diseases: a review of fifteen years of trials for their control with chemicals and biocontrol agents. *Plant Disease* **102**: 1189–1217.

Ouadi, L., Bruez, E., Bastien, S., Vallance, J., Lecomte, P., Domec, J.C., and Rey, P. (2019) Ecophysiological impacts of Esca, a devastating grapevine trunk disease, on *Vitis vinifera* L. *PLoS One* **14**: e0222586.

Peet, R.K. (1974) The measurement of species diversity. *Annual Rev Ecol Syst* **5**: 285–307.

Pinto, C., Pinho, D., Sousa, S., Pinheiro, M., Egas, C., and Gomes, A. (2014) Unravelling the diversity of grapevine microbiome. *PLoS ONE* **9**: e85622.

Pierron, R., Pouzoulet, J., Couderc, C., Judic, E., Compant, S., and Alban, J. (2016) Variations in early response of grapevine wood depending on wound and inoculation combinations with *Phaeoacremonium aleophilum* and *Phaeomoniella chlamydospora*. *Front Plant Sci* **7**: 268.

Redford, A.J., Walters, T.W., Hodges, A.C., Howard, F.W., Truive, M.D. (2010) Screening aid to pests. In A resource for pests and diseases of cultivated palms. Identification Technology Program CPHST PPQ APHUIS USDA; Fort Collins, CO.

Reis, P., Magnin-Robert, M., Nascimento, T., Spagnolo, A., Abou-Mansour, E., Fioretti, C., *et al*. (2016) Reproducing Botryosphaeria dieback foliar symptoms in a simple model system. *Plant Dis* **100**: 1071–1079.

Rezgui, A., Ben Ghnaya-Chakroun, A., Vallance, J., Bruez, E., Hajlaouid, M.R., Sadfi-Zouaoui, N., *et al*. (2016) Endophytic bacteria with antagonistic traits inhabit the wood tissues of grapevines from Tunisian vineyards. *Biol Control* **99**: 28–37.

Sieber, T.N. (2007) Endophytic fungi in forest trees: are they mutualists? *Fungal Biol Rev* **21**: 75–89.

Sun, X., Ding, Q., Hyde, K.D., and Guo, L.D. (2012) Community structure and preference of endophytic fungi of three woody plants in a mixed forest. *Fungal Ecol* **5**: 624–632.

Surico, G., Mugnai, L., and Marchi, G. (2006) Older and more recent observations on esca: a critical overview. *Phytopathol Mediterr* **45**: 68–86.

Surico, G., Mugnai, L., and Marchi, G. (2008) The esca disease complex. In *Integrated Management of Diseases Caused by Fungi, Phytoplama and Bacteria*, Ciancio, A., and Mukerji, K. (eds). Dordrecht: Springer, pp. 119–136.

Wallner, G., Amann, R., and Beisker, W. (1993) Optimizing fluorescent in situ hybridization with rRNA-targeted oligonucleotide probes for flow cytometric identification of microorganisms. *Cytometry* **14**: 136–143.

White, T., Birns, T., Lee, S., and Taylor, J. (1990) *Amplification and Direct Sequencing of Fungal Ribosomal RNA Genes for Phylogenetics. PCR Protocols: A Guide to Methods and Applications*, New York, NY: Academic Press, pp. 315–332.

Zarraonaindia, I., Owens, S.M., Weisenhorn, P., West, K., Hampton-Marcell, J., Lax, S., *et al*. (2015) The Soil Microbiome Influences Grapevine-Associated Microbiota. *Mbio* **6**: e02527–e02514.

Zhang, T., Shao, M.F., and Yé, L. (2012) 454 pyrosequencing reveals bacterial diversity of activated sludge from 14 sewage treatment plants. *ISME J* **6**: 1137–1147.

Supporting Information

Additional Supporting Information may be found in the online version of this article at the publisher's web-site:

Fig. S1 Rarefaction curves illustrating the observed numbers of fungal (A) and (B) and bacterial (C) and (D) (genera in

wood samples obtained from different vine organs/tissues (rootstock, trunk and cordon / non-necrotic and white-rot tissues) and at four different sampling dates (April, June, September 2010 and January 2011).

Fig. S2 DOPE-FISH/CLSM detection of bacteria in non-necrotic woody tissues of trunk from diseased (A-F) and healthy (G-L) grapevines sampled in June 2010. Orange/reddish = specific bacteria, Actinobacteria, Alphaproteobacteria, Gammaproteobacteria, Firmicutes. Green = all non-specific bacteria.

Fig. S3 DOPE-FISH/CLSM detection of bacteria in non-necrotic woody tissues of trunk from diseased (A-F) and healthy (G-L) grapevines sampled in January 2011. Orange/reddish = specific bacteria, Actinobacteria, Alphaproteobacteria, Gammaproteobacteria, Firmicutes. Green = all non-specific bacteria.

Table S1 P-values (P) representing comparison between each sampling date of fungi (A) and bacteria (B) and between fungi (C) and bacteria (D) of the non-necrotic tissue rootstock, trunk and cordon of asymptomatic and symptomatic vines (E) and (F).

Table S2 Results of ANOVA tests comparing different part for healthy or diseasec vines of fungal and bacterial communities (A) and (B) or from fungal or bacterial communities of the different organs (C) and (D). NS = no significant differences.

Table S3 Proportions of the 20 most abundant fungal species of non-necrotic tissue of disease and healthy vines sampled at four seasons (April, June, September and January). Average of all samples of cordon or trunk or rootstock. Sym = symptomatic and Asym = asymptomatic.

Table S4 Proportions of the 20 most abundant bacterial families of non-necrotic tissues of healthy and disease vines sampled at four seasons (April, June, September and January). Average of all samples of cordon or trunk or rootstock. Sym = symptomatic and Asym = asymptomatic.